OVERVIEW OF HIGH POWER VACUUM DRY RF LOAD DESIGNS*

A. Krasnykh, A. Brachmann, F-J Decker, T. Maxwell, and J. Sheppard, SLAC, Menlo Park, USA

Abstract

A specific feature of RF linacs based on the pulsed traveling wave (TW) mode of operation is that only a portion of the RF energy is used for the beam acceleration. The residual RF energy has to be terminated into an RF load. Higher accelerating gradients require higher RF sources and RF loads, which can stably terminate the residual RF power. This overview will outline vacuumed RF loads only. A common method to terminate multi-MW RF power is to use circulated water (or other liquid) as an absorbing medium. A solid dielectric interface (a high quality ceramic) is required to separate vacuum and liquid RF absorber mediums. Using such RF load approaches in TW linacs is troubling because there is a fragile ceramic window barrier and a failure could become catastrophic for linac vacuum and RF systems. Traditional loads comprising of a ceramic disk have limited peak and average power handling capability and are therefore not suitable for high gradient TW linacs. This overview will focus on "vacuum dry" and "all-metal" loads only that do not employ any dielectric interface between vacuum and absorber.

INTRODUCTION

SLAC has been developing next generation accelerator technologies for science, medicine, industry, and homeland security since 1962. Achievement of 100 MeV/m accelerating gradients is one major problem of accelerator technology. SLAC scientists have contributed to this program for many years and the progress in this field is remarkable. One shall recall that high accelerating gradient is a function of the energy stored in the accelerating structure that, in turn, depends on the input RF power. Progress in both: (1) technology of RF accelerating structures and (2) high power RF sources has been substantial. However, another important component in this technology needs to be considered; RF loads which terminate significant residual powers. For traveling wave accelerating structures, the termination problem of residual RF power is directly linked with the development of high gradient structures and multi-Megawatt peak RF sources. The problem of inadequate high power S-Band vacuum dry loads for the SLAC linac exists today (and for the next generation of accelerator technologies) and needs to have a modern technical solution [1].

The LCLS-II [2] installation will employ L-Band superconducting accelerating structures which are housing in the front end of the SLAC linac tunnel. The disassembled hardware could be useful for the LCLS-I warm linac upgrade. Figure 1 shows two layouts.

*Work supported by US Department of Energy contract DE-AC02-76SF00515

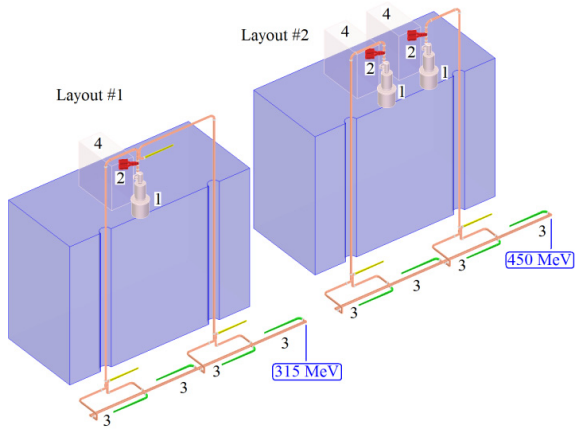

Figure 1: Two station layouts: 1 is 5045 klystron, 2 is SLED cavity, 3 is 10 FT long accelerating structure, and 4 is klystron modulator.

The Layout #1 represents the existing RF configuration of each SLAC klystron station. The 5045 klystron (1) feeds four disk loaded traveling sections (3) through the SLED (2). The typical beam energy gain is approximately 315 MeV per station. A potential LCLS-I upgrade with the disassembled components could be done as it is shown in the Layout #2. This case the FEL X-ray energy could be increased by $\sqrt{2}$ and reach approximately 14 keV. The Layout #2 allows having more headroom and flexibility for the linac operation. However the accelerating gradient in the accelerating structures will be approx. 40 MeV/m and each RF load will absorb approx. 40 MW peak of the residual power. A brief overview of potential RF candidates for SLAC linac is discussed.

OVERVIEW OF VACUUM DRY LOAD DESIGNS

Basically there are two designs. The design based on a usage of lossy ceramics is one concept and the design based on a usage of high resistive metals is another one.

RF Loads with Lossy Ceramic

Figure 2 shows the RF load that was cut in such a way to observe the ceramic wedges [3].

Figure 2: Vacuum dry load with AlN ceramic wedges.

Those lossy ceramic wedges are brazed alongside each narrow waveguide wall. There are water cooling channels at the outside of these walls. The lossy ceramic wedges are aluminium nitride (AlN) loaded with 7% glassy carbon. The array of ceramic wedges is tapered at the front. This is a transition part of the load. After the transition there is an array with a constant thickness. This load was design to terminate a 60 MW peak, approx. 3 kW average with 10% bandwidth at 11.424 GHz centre frequency. The load did not meet the spec due to surface breakdown of wedges.

A similar approach was employed in upgraded RF loads for KEK 2.5 GeV electron linac [4]. Figure 3 shows the load cut-away view.

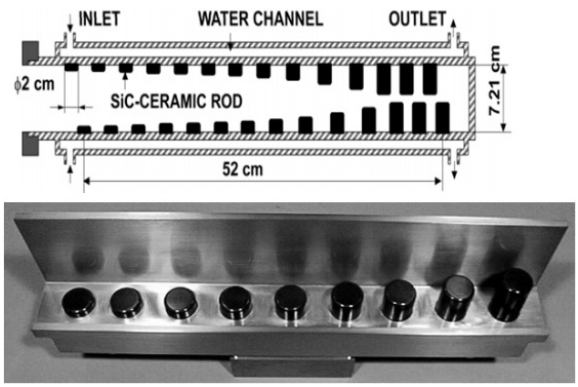

Figure 3: TE10 Vacuum dry load with SiC cylinders.

Commercial available RF loads from Nihon Koshuha Co. contains eight posts only [5]. SLAC bought five loads and only two loads met our specification. A breakdown happened during processing at 25 MW peak, 1 usec pulse width, and 120 Hz (approx. at 3 kW average). After breakdown dust like particles are seen in the areas that are pointed with white arrows (see Figure 4).

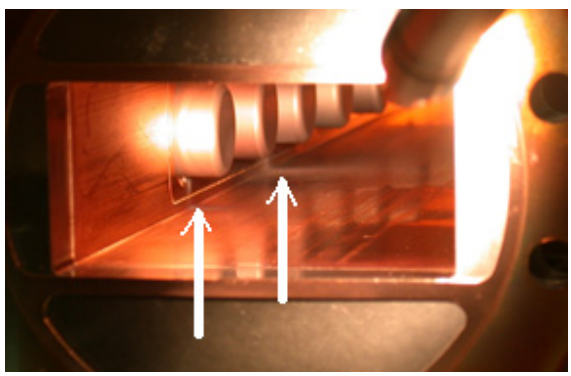

Figure 4: Surface breakdowns on SiC posts.

A detail HFSS analysis showed that surfaces of first SiC posts are electrically overstressed. Our experience with SiC loads shows that the SiC load acceptance rate is rather low [1]. The commercially available SiC loads apparently overstressed vs. the original design where the number of SiC posts per each narrow waveguide wall were reduced by a factor 1.75.

Muons Inc. has proposed the RF load (see Figure 5) where custom porcelain doped with SiC powder is used [6].

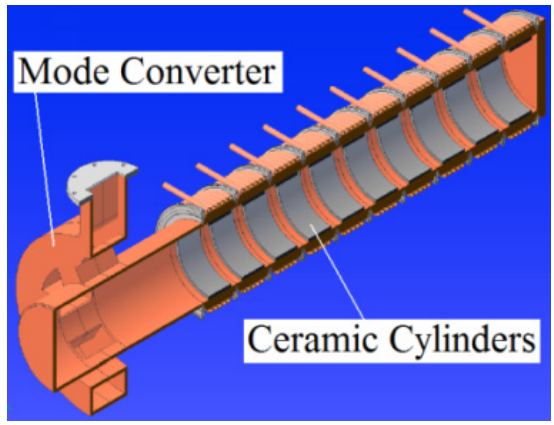

Figure 5: TE01 vacuum dry load with ceramic cylinders.

In order to avoid the ceramic breakdown the working mode in the RF load is TE01. The TE10-TE01 mode converter is needed. The design has been completed. High power tests are expected.

"All-metal" RF Loads

There are several type materials which are used in high power load designs. Typically they are stainless steel SS430, Kanthal, and Nichrome. Kanthal and SS430 are mainly used in all-metal designs. A matrix composition of Kanthal is similar to the SS430 composition except for the Al content. There is a belief that a very thin film of alumina may keep the amount of Fe and Cr components from combusting in air even at its melting temperatures. The RF surface resistivity of the absorber layer depends on this amount.

A 100 MW peak, 8 kW average RF load with the SS430 RF absorber is shown in Figure 6 [7] and [8]. A pulse TE10 mode RF power is propogated in a rectungular waveguide. However an RF termination is based on a lossy cylindrical waveguide operating in the TE11 mode.

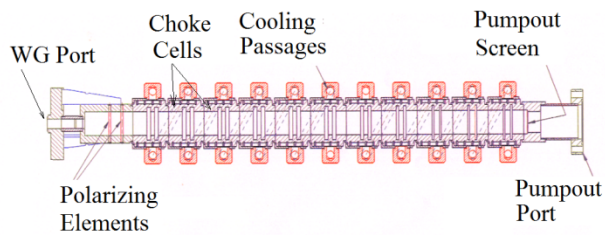

Figure 6: RF load cross section with functional parts.

The main reason to use a TE11 mode in a cyilindrivcal waveguide is to create an RF absorption that is azimuthally uniformly distributed in an array of low-Q radial lines (i.e. choks). A pair chokes were designed in resonance (i.e. the choks deps is ~λ/4). The radial extent and axial length of the choke slots determine the RF power loss. A circular polarizer is used at the front end of the load to rotate of the TE11 mode while the RF power propagates from the input port to the load end. The second reason to employ TE11 mode is the fact that the peak of the electric field for this mode is lower. Sizes of each choke-pair are different from one pair to another.

ISBN 978-3-95450-147-2

The CERN 50 MW peak (300 nsec) dry RF load is shown in Figure 7.

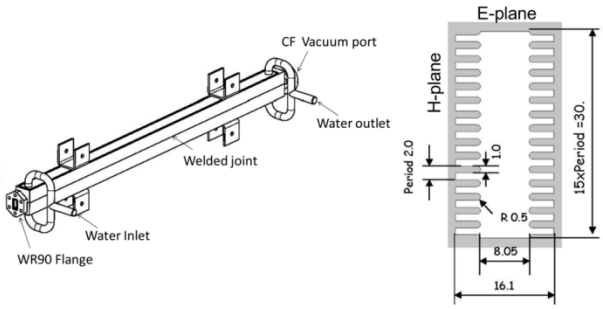

Figure 7: Stainless steel vacuum dry RF load [9].

The whole RF load is made from SS430 material. This load consists four major parts. After a standard rectangular waveguide flange, sizes of the waveguide H-plane walls are smoothly increased (a tapered part). After that there is a regular part. A matching section is needed between the end of the tapering and regular part. The regular part of the load contains an array of wedges (kerfs) on the H-plane waveguide walls. The working mode is TE10 although the mode propagates in oversized taper, matching, and regular waveguide parts. The efficiency of the RF power absorption mainly depends on two parameters: (1) surface resistivity of the SS430 steel and (2) the number and sizes of wedges. The wedges increase the effective surface resistance and attenuation rate accordingly.

An original SLAC linac RF load designed to terminate 2-3 MW peak power using 200 um of coated Kanthal material as the high power absorber [10]. Kanthal wire was flame-sprayed onto a stainless steel. It has been found that the RF amplitude and phase of terminated power are unstable. It has shown that these RF instabilities are associated with the processes inside of the RF load vacuum envelope. The new RF load has been designed and tested [11]. The RF load cross section is shown in Figure 8.

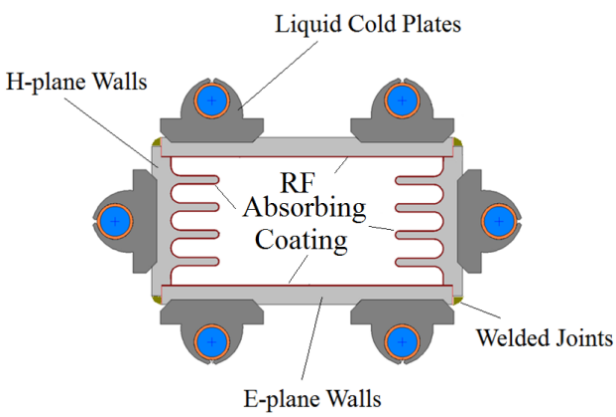

Figure 8: Aluminium alloy waveguide with a thermal spray coat as a high power vacuum dry RF load.

More details concerning this design the reader could find in [11] and [12]. A special thermal spray technology (a different to the previous wire flame spray technology) was employed for the formation of the RF absorber layer capable of dissipating stably and reliably a 30+ MW peak (4+ kW average) RF power with an acceptable ultra-high vacuum outgassing rate. A life time study of this approach will be performed at SLAC linac during this year.

CONCLUSION

A brief overview of multi MW peak vacuum dry load designs is discussed. Two concepts were considered: (1) designs based on the usage of lossy ceramic and (2) designs based on "all-metal" approach. The "all-metal" designs are a cost effective and reliable to terminate stably a residual RF lower in the traveling wave accelerating structures.

REFERENCES

[1] A. Krasnykh et al., *Proc. LINAC'12* and SLAC-PUB-15229.

[2] https://www6.slac.stanford.edu/files/Strategic_Plan_2014.pdf

[3] K. Ko et al., *Proc. PAC'95*, v. 3, p. 1726.

[4] H. Matsumoto et al., *Proc. PAC'99*, p. 842.

[5] http://www.nikoha.co.jp/eg/egindex.html

[6] M. Neubauer et al., *Proc. PAC'13*, Pasadena, p. 975.

[7] S. Tantawi and A Vlieks, SLAC-PUB-6826.

[8] W. Fowkes et al., *Proc. PAC'97*, p. 3189.

[9] M. Matsumoto et al., *Proc. LINAC'10*, p. 226, Tsukuba, Japan.

[10] "The Stanford Two-Mile Accelerator", pp. 376-381, R. B. Neal, General Editor, 1968, W. A. Benjamin, Inc., NY, Amsterdam.

[11] A. Krasnykh, SLAC-TN-15-037.

[12] A. Krasnykh, SLAC-WP-129.